European Conference on Computational Fluid Dynamics
ECCOMAS CFD 2006
P. Wesseling, E. Oñate and J. Périaux (Eds)

A LAGRANGIAN SIMULATION METHOD FOR SUSPENSIONS IN VISCOELASTIC FLUIDS

Ahamadi Malidi*, Oliver Harlen†

Department of Applied Mathematics
University of Leeds,Woodhouse lane, Leeds, LS2 9JT, United Kingdom
*e-mail: malidi@maths.leeds.as.uk
web page: http://www.maths.leeds.ac.uk/∼ malidi/
† e-mail: oliver@maths.leeds.as.uk

Key words: Viscoelastic fluid, suspensions, Lagrangian methods, finite element method

Abstract. *We present a novel Lagrangian finite element method for simulating suspensions of particles in viscoelastic fluids. We solve the flow in a unit cell containing a small number of particles with doubly periodic boundary conditions on a self-replicating two-dimensional lattice to replicate a suspension on an infinite domain. The method uses a Lagrangian finite element grid that deforms with fluid combined with a quotient representation of the periodic lattice.*

We show that qualitatively different results are obtained for the shear-thinning pompom constitutive equation compared to those obtained using the Oldroyd B fluid. For the pompom fluid we show that the changes to shear viscosity with the addition of particles can be obtained by a simple shifting of the shear-rate and shear-stress.

1 INTRODUCTION

In many polymer processing applications filler particles such as glass beads are added to the polymer matrix. One approach to studying the rheology of such multiphase systems is to perform direct simulations of the motion of the suspended particles when subjected to an external flow. In studying the bulk rheology of a suspension it is convenient to consider an infinite domain of suspension undergoing homogenous shearing flow. In numerical simulations the infinite domain is replaced by a spatially periodic structure based upon a unit cell containing a limited number of particles. Under shear flow these unit cells slide relative to one another and this relative momement must be taken account of in applying the periodic boundary conditions [10].

Hwang *et. al.*[7] developed a simulation technique for sheared suspensions in Newtonian fluids based on the distributed Lagrangian multiplier method of Glowinski *et. al.*[5] by using Lagrangian multipliers to impose both the sliding biperiodic boundary conditions and the boundary conditions at the particle surface. In a subsequent paper they extended

this technique to viscoelastic fluids described by the Oldroyd B equation [8]. This allows the solution to be solved on a fixed grid.

In this paper we describe an alternative approach based upon a Lagrangian simulation in which the grid deforms with the fluid. This approach was pioneered for viscoelastic fluids by Rassmussen and Hassager [13] and has the advantage that the constitutive equation is solved in its natural frame. Our method is based upon the Lagrangian-Eulerian method of Harlen *et. al.*[6], which uses Delaunay reconnections to preserve grid quality. In this application we enforce the periodic boundary conditions using a quotient space representation in which each point in the unit cell is replicated at corresponding image points in the lattice. Another advantage of using this approach is that the connectivity of the grid then automatically enforces the correct periodic boundary conditions.

In analysing the effect of fillers on the nonlinear shear properties of viscoelastic fluids we consider two different viscoelastic constitutive equations. In order to benchmark our results with those of Hwang *et. al.*[8], we consider the Oldroyd B constitutive equation. In the absence of particles this constitutive model has a constant shear viscosity and the addition of particles produces a shear-thickening fluid. This behaviour is not typical of polymer melts, which are strongly shear-thinning, and to investigate these we consider the pom-pom constitutive model of McLeish and Larson [12] which is a more appropriate model for polymer melts. For the pompom fluid we find that the changes in the shear viscosity can be accounted for by a simple shifting of the shear-rate and shear-stress.

2 FLOW GEOMETRY

The idealised problem we wish to consider is a two-dimensional unbounded domain containing hard particles suspended in polymeric fluid under simple shear flow. However, in order to make the computations tractable we approximate this domain by a periodically replicated unit cell of size $H \times L$, containing N particles. Under the action of a shear flow each cell within the lattice translates along the shear direction so that the cells slide relative to on another as illustrated in figure 1. The particles are also able to move across the cell boundaries. To implement this periodic structure we define an equivalence class of points in the infinite domain $\Omega^{inf}(t)$ that correspond to the same point in the unit cell, $\Omega(t)$,

$$S(t) = \{(x_{image}, y_{image}) = (x_{cell} + n\gamma H + mL, y_{cell} + nH)\}. \tag{1}$$

Here the integer pair (m, n) denotes the shift in the periodic image and γ the shear strain, $\gamma = \dot{\gamma}t$. (For numerical convenience the strain maybe reset to zero after each period of the lattice, $L/(H\dot{\gamma})$) The original unit cell corresponds to the points $m = 0, n = 0$ except for points on the top and righthand edges, which are respectively the $n = 1$ and $m = 1$ images of the points on the bottom and lefthand edges. Figure 2 shows an illustration of a very simple mesh of this form consisting of eight triangular elements connecting four replicated points and their appropriate images. Note that after one strain period the unit cell may be recovered by choosing appropriate images.

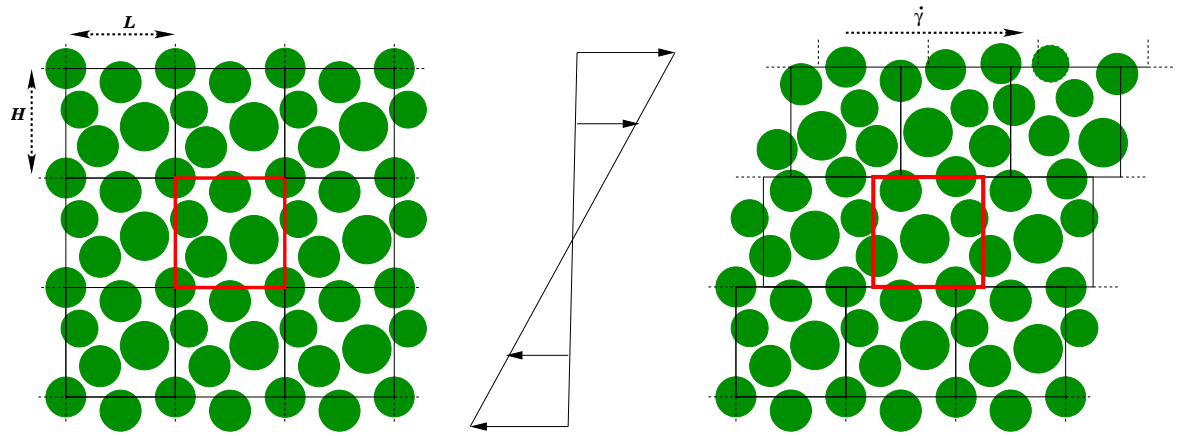

Figure 1: Sketch illustrating the relative motion of the cells in a biperiodic lattice under shear flow.

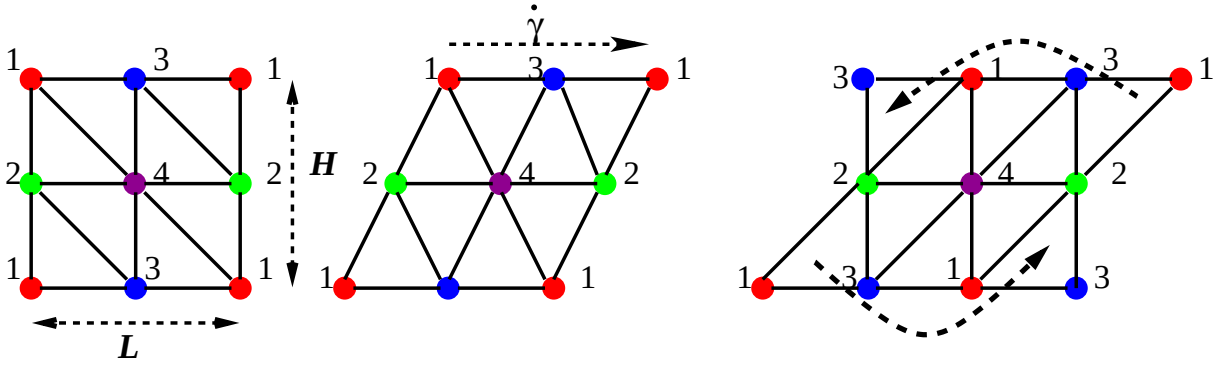

Figure 2: Sketch showing a simple example of a unit cell made up of eight triangular elements formed from joining four points and their appropriate images. After one strain period the original unit cell may be recovered by choosing appropriate images.

The external shear flow is imposed by the condition that the velocity of the (m, n) image is given by

$$\mathbf{u}(x_{image}, y_{image}) \longrightarrow \mathbf{u}(x, y) + m(\dot{\gamma}H, 0), \tag{2}$$

while all other variables, including those governing polymer microstructure are the same at each image point. The unit cell is divided into triangular finite elements labelled by the vertex points. As each vertex moves with the fluid velocity the biperiodic structure is maintained by the grid connectivity.

3 GOVERNING EQUATIONS

The flow is assumed to be incompressible, isothermal and interialess, so that the equations of conservation of mass and momentum are given by,

$$\begin{cases} \nabla \cdot \boldsymbol{\sigma} &= 0 \\ \nabla \cdot \mathbf{u} &= 0, \end{cases} \tag{3}$$

where $\mathbf{u}$ is the fluid velocity and $\boldsymbol{\sigma}$ is stress tensor. For a polymeric fluid the stress is of the form

$$\boldsymbol{\sigma} = -p\mathbf{I} + \mathbf{2}\mu_{\mathbf{s}}\mathbf{D} + \boldsymbol{\sigma}^{\boldsymbol{P}}, \tag{4}$$

where p is the pressure, $2\mu_s\mathbf{D}$ is the Newtonian stress due to any low molecular weight solvent or fast relaxing modes which has a viscosity μ_s and $\boldsymbol{\sigma}^P$ is the viscoelastic component. The form of $\boldsymbol{\sigma}^P$ is dictated by the choice of constitutive equation. Differential constitutive equations are of the generic form

$$\boldsymbol{\sigma}^P = \mathcal{G}(\mathbf{T}), \tag{5}$$

where $\mathbf{T}$ is a set of internal variables describing the microstructure. These variables evolve as a consequence of the local strain-rate history of the fluid element and so satisfy an evolution equation of the generic form

$$\frac{D\mathbf{T}}{Dt} = \mathcal{F}(\mathbf{T}, \nabla\mathbf{u}). \tag{6}$$

This is a hyperbolic equation with characteristics given by the particle paths.

4 CONSTITUTIVE EQUATIONS

In this study we consider two particular constitutives equations, the Oldroyd B and pompom models. The Oldroyd-B model may be derived from the kinetic theory of a suspension of linear elastic dumbbells [3]. The viscous drag on the molecule is represented by the drag on the dumbbell ends and the entropic force restoring the molecule to an equilibrium configuration is represented by a Hookean spring. The polymeric stress $\boldsymbol{\sigma}^P$ is given by

$$\boldsymbol{\sigma}^P = G(\mathbf{A} - \mathbf{I}), \tag{7}$$

where G is the elastic modulus and the second rank tensor $\mathbf{A}$ is the second moment of the dumbbell end-to-end vector distribution. The evolution equation for $\mathbf{A}$ corresponding to equation (6) is given by

$$\overset{\triangledown}{\mathbf{A}} = -\frac{1}{\tau}\Big(\mathbf{A} - \mathbf{I}\Big), \tag{8}$$

where

$$\overset{\triangledown}{\mathbf{A}} = \frac{\partial\mathbf{A}}{\partial t} + \mathbf{u}\cdot\nabla\mathbf{A} - \mathbf{A}\cdot\nabla\mathbf{u} - (\nabla\mathbf{u})^T\cdot\mathbf{A} \tag{9}$$

is the *upper convected* time derivative of the $\mathbf{A}$, and τ is the relaxation time of the polymer. In steady shear flow the shear stress in this fluid at steady state is equal to $(\mu_s + G\tau)\dot{\gamma}$ so that this fluid has a constant shear viscosity of $\mu_s + G\tau$. However, it also possesses a postive normal stress difference $N_1 = \sigma_{xx} - \sigma_{yy} = 2G\dot{\gamma}^2\tau^2$.

This model has three parameters, the solvent viscosity μ_s, the relaxation time τ and the elastic modulus G from which we can obtain two dimensionless groups: the Weissenberg

number $We = \dot{\gamma}\tau$ measures the ratio of the shear-rate to the relaxation rate of the fluid; and $\beta = G\tau/(\mu_s + G\tau)$ measures the fraction of the shear viscosity contributed by the polymer. The limits $We \to 0$ or $\beta \to 0$ correspond to a Newtonian fluid, while the limit $\beta = 1$ is the upper convected Maxwell model.

Dumbbells models such as the Oldroyd B model ignore intermolecular interactions and so are strictly only applicable to dilute polymer solutions. In concentrated solutions and melts the motion of single polymer is constrained by its neighbours, which introduces new physics into the constitutive equation. A simple model that includes these effects is the pompom model introduced by McLeish and Larson [12]. We will use the differential version of the original pompom model, but with the modification introduced by Blackwell *et al* [4]. The model is obtained by considering a melt of 'pompom' molecules formed by connecting two q-armed star polymers with a backbone chain. The presence of the branch points at the ends of the backbone chain inhibits its motion along its tube, so that stretch and orientation relaxation times of the backbone, τ_s and τ respectively, are controlled by the relaxation of the star arms. We shall consider a single pompom mode together with a solvent term so that

$$\boldsymbol{\sigma}^P = 3G\lambda^2 \frac{\mathbf{A}}{\mathrm{Tr}(\mathbf{A})}. \tag{10}$$

The tensor $\mathbf{A}$ remains given by equation (8) where τ is now the orientation relaxation time, while the backbone stretch, λ, is given by

$$\frac{D\lambda}{Dt} = \frac{\lambda}{\mathrm{Tr}\mathbf{A}}\mathbf{A} : \nabla\mathbf{u} - \frac{e^{2(\lambda-1)/q}}{\tau_s}(\lambda - 1), \tag{11}$$

up to the maximum stretch, q. We use the same non-dimensionalisation used for the Oldroyd B model, so that the Weissenberg number is based upon the orientation relaxation time, τ. We now have two additional dimensionless groups: q, the number of arms and $We_s = We\tau_s/\tau$, the Deborah number based upon the stretch relaxation time. This fluid also has a positive first normal stress difference, but unlike the Oldroyd B model it is strongly shear-thinning.

5 PARTICLES

The filler particles are assumed to be rigid circular particles that are force and couple free. Assuming that there is no slip between the filler particles and the matrix the fluid velocity at the surface of particle i is given by

$$\mathbf{u} = \mathbf{U_i} + \boldsymbol{\Omega_i} \times (\mathbf{x} - \mathbf{X_i}), \tag{12}$$

where $\mathbf{U_i}$ and $\boldsymbol{\Omega_i}$ are the unknown velocity and angular velocity of the particle. To enforce these boundary conditions we introduce a surface force density $\mathbf{f^i}(s)$ around the surface of the particle i which acts as a Lagrange multiplier to force the fluid inside particle i

to behave as a rigid solid. The angular velocity $\mathbf{\Omega}_i$ and velocity $\mathbf{U_i}$ are found from the conditions of no net force and torque on each particle,

$$\mathbf{F^i} = \int_{\partial P_i} \mathbf{f^i}\, ds = 0, \tag{13}$$

$$\mathbf{T^i} = \int_{\partial \mathbf{P_i}} (\mathbf{x} - \mathbf{X_i}) \times \mathbf{f^i}\, \mathbf{ds} = \mathbf{0}. \tag{14}$$

The average stress in the suspension can be found using the formula given by Batchelor [2],

$$< \boldsymbol{\sigma} >= \frac{1}{V}\Big[\int_{V_f} \boldsymbol{\sigma} dV_f + \sum_{particles} \mathbf{S^i}\Big] \tag{15}$$

where V_f is the volume of the fluid phase and $\mathbf{S^i}$ is the particle stresslet from particle i given by

$$S^i_{jk} = \frac{1}{2}\int_{\partial P_i} \Big[(x_j - X_j) f_k + f_j (x_k - X_k) ds\Big]. \tag{16}$$

6 NUMERICAL METHOD

The numerical method is based on the split Eulerian-Lagrangian technique of Harlen *et. al.*[6]. In this method we first find the fluid velocity and pressure for the current values of microstructural variables $\mathbf{A}$, λ and positions of the particles. We then step forward in time to find the new values of $\mathbf{A}$, λ and particle positions.

We follow Glowinski *et. al.*[5] by using the combined equation of motion to derive the weak form of the governing equations (3), (12), (13) and (14). The natural combined velocity spaces for the fluid and particles equations is given by

$$\begin{aligned} \mathbb{V} \quad &= \{(\boldsymbol{v}, V_i, \xi_i) | \boldsymbol{v} \in H^1(\Omega))^2, V_i \in \mathbb{R}^2, \xi_i \in \mathbb{R}, \\ &\qquad \boldsymbol{v} = V_i + \xi_i \times (x - X_i) \text{ in } P_i(t), \text{ and } \boldsymbol{v} \text{ biperiodic on } \partial\Omega\}, \end{aligned} \tag{17}$$

In the distributed Lagrange multiplier method the extended weak form for whole domain can be obtained by removing the constraint (12) from the velocity space and enforcing it weakly as a side constraint. This is done by introducing a Lagrange multiplier, which can be interpreted as an additional surface force required to maintain the rigid-body motion of particle $P_i(t)$. In our methodology the constraints (13) and (14) are used to determine the unknown $\mathbf{U_i}$ and $\mathbf{\Omega_i}$ and therefore they must be incorporate into the final weak form.

For a given finite element mesh, the discretisation of the weak form of equations (3), (12), (13) and (14) leads to a symmetric indefinite linear system of algebraic equations. These are solved using a preconditioned conjugate residuals method with block preconditioner of the form suggested by Silvester & Wathen [16].

The microstructure variables $\mathbf{A}$ and λ are updated using a first-order time-step in a frame which is deforming with the fluid. The vertices of the triangles are material

points and so each triangle is a material volume. Consequently, the fluid strain within each triangle can be found from its deformation. The sides of the triangles are material line elements, so they rotate and stretch as co-deforming vectors. Hence we can choose vectors $\mathbf{p}$, $\mathbf{q}$ along two sides of the triangle as base vectors in a codeforming frame. In these triangle $(\mathbf{p}, \mathbf{q})$ coordinates, the components of $\mathbf{A}$ and the identity tensor $\mathbf{I}$ are given by

$$\tilde{\mathbf{A}} = Q^{-1}\mathbf{A}\{Q^{-1}\}^{\dagger} \qquad \tilde{\mathbf{I}} = Q^{-1}\{Q^{-1}\}^{\dagger} \tag{18}$$

respectively, where the Q is the transformation matrix from the co-deforming to the Eulerian frame. In the codeforming frame, the evolution equation (8) for $\tilde{\mathbf{A}}$ is

$$\frac{d\tilde{\mathbf{A}}}{dt} = -\frac{1}{\tau}\left(\tilde{\mathbf{A}} - \tilde{\mathbf{I}}\right). \tag{19}$$

Thus the constitutive equation is reduced to a simple ordinary differential equation.

A grid which is fixed in the fluid will be distorted by velocity gradients within the fluid, which will ultimately degrade the accuracy of the finite element solution. To overcome this without having to resort to introducing an entirely new mesh we employ the following methods of grid improvement.

1. At each time step the existing nodes are reconnected where necessary to form a Delaunay triangulation, using an iterative algorithm.

2. Edges shorter than a minimum length are removed by removing one of the nodes.

3. Triangles with areas greater than a maximum area are split by introducing a new node at the centroid.

4. After any addition or deletion of nodes the Delaunay triangulation is restored by running the iterative algorithm again.

When particles become close together the minimum length and maximum area measures in the region between the particles is reduced so as to increase the resolution in this region. However, even with increased resolution it proves necessary to include a short-range repulsive force between particles to prevent overlap.

7 RESULTS AND DISCUSSION

The main rheology measurements of interest are the average shear stress $< \sigma_{xy} >$ and average first normal stress difference $< N_1 > = < \sigma_{xx} - \sigma_{yy} >$. For the Oldroyd B model we can compare these to the values obtained from the fluid alone by defining the average relative viscosity as,

$$\eta = \frac{< \sigma_{xy} >}{(\mu_s + G\tau)\dot{\gamma}},$$

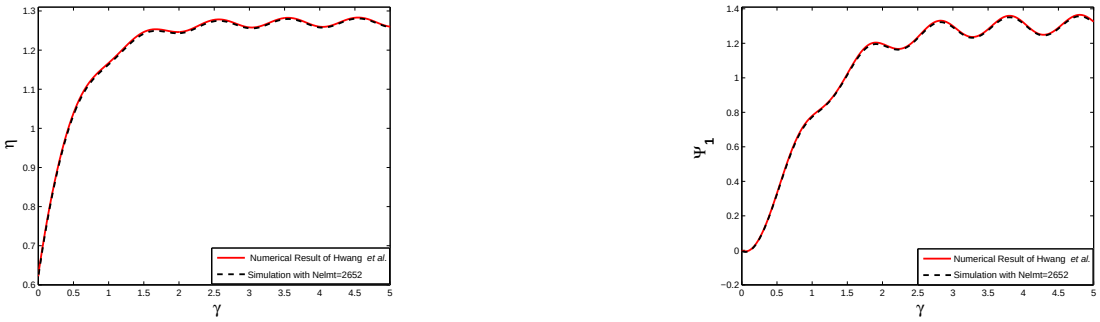

Figure 3: Comparison of our results for a mesh with 2652 elements and timestep 0.005 to results obtained by Hwang *et. al.*(in fig 4 of reference [8]) for $We = 0.5$ and $\beta = 0.5$.

and average relative first normal stress difference coefficient as

$$\Psi_1 = \frac{< \sigma_{xx} - \sigma_{yy} >}{2G\tau^2\dot{\gamma}^2},$$

so that in the absence of particles both η and Ψ_1 tend to unity as $t \to \infty$. We first consider the case of a single particle of radius $r = 0.2$ at the centre of a square cell of unit length. This case was also studied by Hwang *et. al.*[8] and so provides us with a means of benchmarking our code. In figure 3 we compare our results for η and Ψ_1 to those obtained by Hwang *et. al.* for $We = 0.5$ and $\beta = 0.5$. Our results were obtained with a mesh containing 2652 elements and a timestep of 0.005 and are in excellent agreement with those published by Hwang.

In figure 4 we show the variation in the results for η and Ψ_1 for different values of the Weissenberg number. For a Newtonian fluid there is an oscillation in the relative viscosity caused by the periodic variation in the cellular structure. For non-zero Weissenberg numbers this is superimposed on the usual viscosity increase at start-up seen with the Oldroyd fluid. Note that the eventual steady state oscillation is above that of a Newtonian fluid indicating that the shear viscosity is increasing with Weissenberg number. This shear-thickening behaviour has been recently reported by Scirocco *et. al.*[15] for polystyrene spheres suspended in Boger fluids. (A Boger fluid is a dilute solution of a very high molecular weight polymer in a highly viscous solvent, producing an viscoelastic fluid with an almost constant shear viscosity whose rheology is close to that of an Oldroyd B fluid). The average value of the relative first normal stress difference also increases with Weissenberg number, while the magnitude of the oscillations decreases. The latter is the result of the definition of Ψ_1 which is inversely proportional to We squared.

The shear-thickening and increases in first normal stress difference with the addition of particles is a consequence of the way the particles modify the flow field. The velocity gradient $\nabla\mathbf{u}$ can be decomposed into the sum of a symmetric strain-rate tensor $\mathbf{D}$ and an anti-symmetric vorticity tensor $\boldsymbol{\zeta}$. In simple shear flow the magnitudes of $\mathbf{D}$ and $\boldsymbol{\zeta}$ are equal so that the averages of $\mathbf{D}$ and $\boldsymbol{\zeta}$ over the whole domain of the fluid plus the particles

must be equal. However, while the interior of the particles is strain-free the particles are free to rotate and so the vorticity inside the particles is non-zero. Consequently in order to maintain the global balance the magnitude of the strain-rate must be larger than the vorticity in the fluid. This change in the strain-vorticity balance in the fluid has a very strong influence on the viscoelastic stress, since fluid particles separate exponentially in a strain-rate dominated flow causing dumbbells to become highly extended.

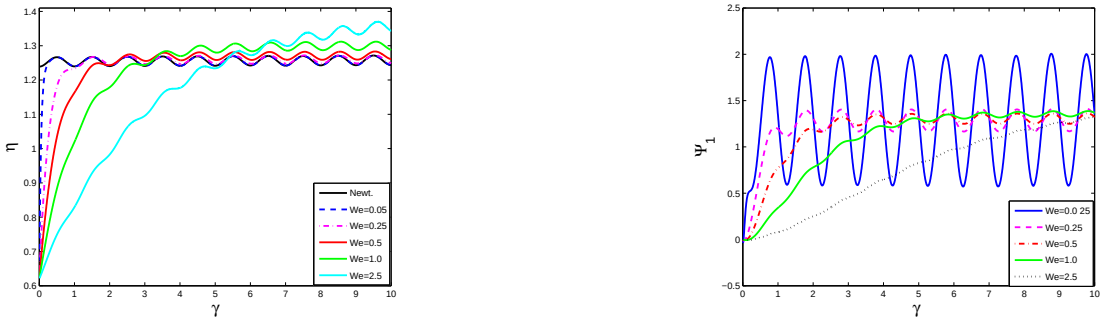

Figure 4: Plot of the relative shear viscosity and first normal stress coefficient as a function of strain $\gamma = \dot{\gamma}t$ for an Oldroyd B fluid with $\beta = 0.5$ for a particle size of $r = 0.2$.

A question arises as to whether this transition phenomenon also occurs in other constitutive models, particularly those more appropriate to polymer melts such as the pompom model. For the pompom model there are no analytic solutions available for the stress in simple shear flow, so rather than showing the relative viscosity and first normal difference we will plot the values of $< \sigma_{xy} >$ and $< N_1 >=< \sigma_{xx} - \sigma_{yy} >$ relative to the Newtonian shear stress $\mu_s\dot{\gamma}$. To obtain steady state values for these quantities we average over the period of oscillation after the steady state regime has been established. In figure 5 we show the average steady state shear and normal stress differences as a function of We for two different particle radii, $r = 0.2$ and 0.3 corresponding to particle area fractions $\Phi = 0.1257$ and $\Phi = 0.2827$ respectively. In this figure we have chosen $G\tau = 3\mu_s$, $q = 2$ and $We_s = 0.5We$. However, we find virtually no effect of the values of q or We/We_s on the results (for $q > 1$ and $We_s < We$). This is because the parameters q and We_s control the evolution of the backbone stretch, λ, but in this model, unlike the Oldroyd B fluid, there is little if any molecular extension taking place and in most of the fluid λ is close to unity.

In contrast to the case of the Oldroyd B fluid, where the greatest increase in viscosity occurred at high Weissenberg numbers, with the pompom model the largest increase in viscosity occurs in the Newtonian limit. Also, whereas before we saw an increase in normal stress difference with the addition of particles for the pompom model this is only true for Weissenberg numbers less than unity. At higher Weissenberg numbers the normal stress difference descreases with the addition of particles. The pompom model show the same qualitative changes in rheology seen in experiments on shear-thinning polymeric fluids (as

opposed to Boger fluids), which were recently reviewed by Barnes [1].

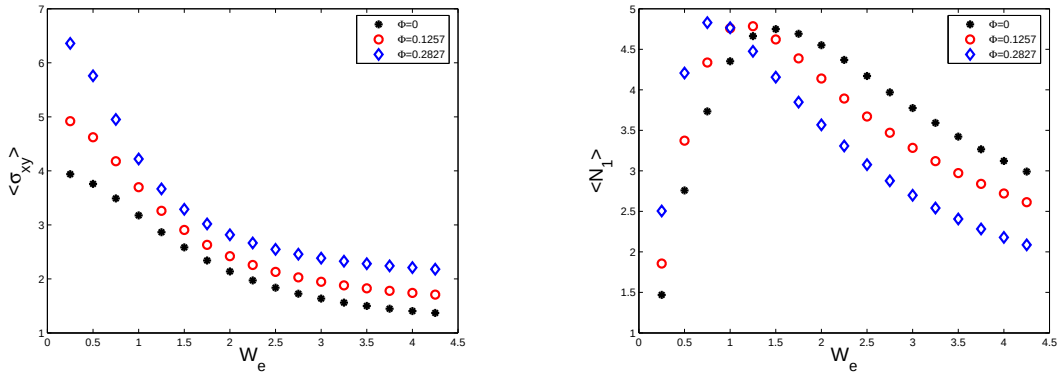

Figure 5: Plot of the steady state shear stress $< \sigma_{xy}$ and first normal stress difference $< N_1 >=< \sigma_{xx} - \sigma_{yy} >$ as a function of Weissenberg number for different particle concentrations for the pompom model with $G\tau = 3\mu_s$, $We_s = 0.5We$ and $q = 2$.

A highly desirable objective of these simulations is to find a simple way of accounting for the effects of adding particles on the fluid rheology. In his review Barnes notes that the effect of adding particles to a shear-thinning fluid is both to shift the shear viscosity upwards, but also to shift the onset of shear-thinning to lower shear-rates, so that a simple vertical shift in viscosity such as that used for suspensions in Newtonian fluids is insufficient. To overcome this we will attempt to superimpose the data for different values of Φ by shifting both the viscosity and shear-rate.

As discussed above, the strain-rate within the particles is zero, and so consequently the average strain-rate in fluid must be larger by a factor of $1/(1-\Phi)$. Thus the effective Weissenberg number in the fluid is

$$We_{\text{eff}} = \frac{We}{(1-\Phi)}. \tag{20}$$

If we also divide $< \sigma_{xy} > /\mu_s\dot{\gamma}$ by the relative change in viscosity of a Newtonian fluid, $\mu(\Phi)/\mu_s$ then we find that the shear stress data for different values of Φ do indeed superimpose, as can be seen in figure 6. This figure also shows the effect of applying the shear-rate, but not the shear-stress shift, to the first normal stress difference. However, the superposition is less convincing in this case.

The apparent success of this simple shifting model for the pompom fluid appears to contradict the results for the Oldroyd model where shear-thickening is observed. While the Oldroyd B model is very sensitive to the balance between straining and vorticity, the pompom model is not because it is only velocity gradients in the direction of the backbone orientation that can produce extension. This is confirmed by our results for other constitutive models that show a distinction in behaviour between dumbbell based constitutive equations such as the Oldroyd model and tube-theory models like the pompom fluid.

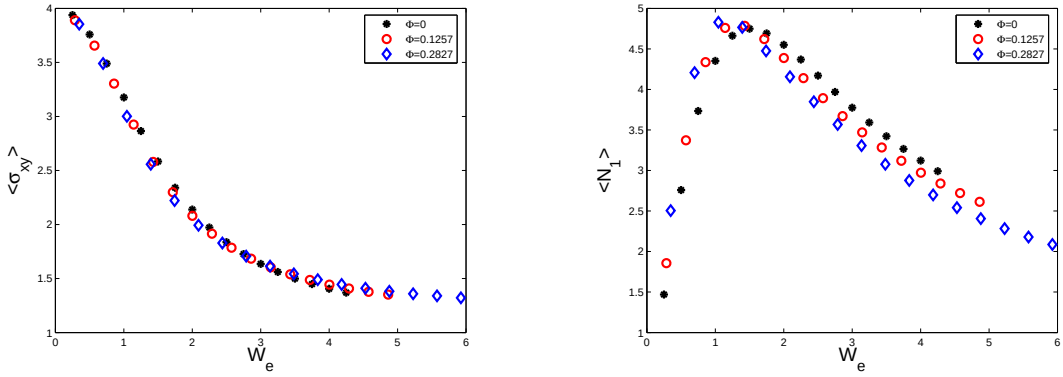

Figure 6: Plot showing the effect of the shifting the steady state shear stress results of figure 5 using the effective Weissenberg number defined in equation (20) and scaling the shear viscosity with the relative change in the Newtonian viscosity. The righthand figure shows the first normal stress difference plotted against effective Weissenberg number.

8 CONCLUDING REMARKS

Although all the results described in this paper are for a single particle per unit cell we can also perform simulations with multiple particles per cell. The results for multiparticle simulations are harder to analyse because the structure is no longer replicated periodically. However, such simulations can be used to investigate the phenomenon of particle chaining observed by Lyon *et. al.*[11]. Intriguingly Scirocco *et. al.*[14] did not observe chaining in Boger fluids, but only in shear-thinning fluids. Our numerical method can also be used to study the rheology of suspensions under planar extensional flow, by using the spatially periodic lattice structure of Kraynik and Reinelt [9]. Work on both these fronts is currently underway. It is also possible to extend this method to non-rigid filler particles such as elastic particles or droplets. The current method is however limited to two dimensional simulations while the real systems are three-dimensional. Fully three-dimensional calculations are challenging but may be necessary particularly for investigating interactions between particles such as those responsible for chaining.

ACKNOWLEDGEMENT

We are grateful to the EPSRC for financial support through grant GR/T11807/01.

REFERENCES

[1] H.A. Barnes. The rheology of filled viscoelastic systems: A review, *Rheology Reviews 2003*,1–36, (2003).

[2] G.K. Batchelor. The stress system in a suspension of force-free particles. *J. Fluid Mech.*, **41(3)**, 545–570, (1970).

[3] R.B. Bird, R.C. Armstrong and O. Hassager. Dynamics of Polymeric Fluids, Volume 1. *John Wiley and Sons*, (1987).

[4] R. Blackwell, T.C.B.McLeish and O.G. Harlen. Molecular drag-strain coupling in branched polymer melts. *J. Rheology*, **44**,121–136, (2000).

[5] R. Glowinski, T.-W. Pan, T.I. Hesla and Joseph. A distributed Lagrange multiplier/fictitious domain method for particulate flows. *Int. J. Multiphase Flow*, **25**, 755–794, (1999).

[6] O.G. Harlen, J.M. Rallison and P. Szabo. A split Lagrangian-Eulerian method for simulating transient viscoelastic flows. *J. Non-Newtonian Fluid Mech.*, **60**, 81–104, (1995).

[7] W.R. Hwang, M.A. Hulsen and H.E.H. Meijer. Direct simulation of particle suspensions in sliding bi-periodic frames. *J. Comp. Phys.*, **194**, 742–772, (2004).

[8] W.R. Hwang, M.A. Hulsen and H.E.H. Meijer. Direct simulation of particle suspensions in a viscoelastic fluid in sliding bi-periodic frames. *J. Non-Newtonian Fluid. Mech.*, **121**, 15–33, (2004).

[9] A.M. Kraynik and D.A. Reinelt. Extensional motions of spatially periodic lattices. *Int. J. Multiphase flow*, **18**, 1045–1059, (1992).

[10] A.W. Lees and S.F. Edwards. The computer study of transport processes under extreme conditions. *J. Phys. C*, **5**, 1921-1929, (1972).

[11] M.K. Lyon, D.W. Mead, R.E. Elliott and L.G. Leal. Structure formation in moderately concentrated viscoelastic suspensions in simple shear flow. *J. Rheology*, **45**, 881-890 (2001).

[12] T.C.B. McLeish and R.G. Larson. Molecular constitutive equations for a class of branched polymers: The pom-pom polymer. *J. Rheology*, **42(1)**, 81–110, (1998).

[13] H.K. Rasmussen and O. Hassager. Simulation of transient viscoelastic flow. *J. Non-Newtonian Fluid Mech.*, **46**, 63–99, (1993).

[14] R. Scirocco, J. Vermant and J. Mewis. Effect of the viscoelasticity of the suspending fluid on structure formation in suspensions. *J. Non-Newtonian Fluid Mech.*, **117**, 183–192, (2004).

[15] R. Scirocco, J. Vermant and J. Mewis. Shear thickening in filled Boger fluids. *J. Rheology*, **49**, 551–567, (2005).

[16] D. Silvester and A. Wathen. Fast iterative solution of stabilised Stokes systems. Part 2: using general block preconditioners. *SIAM J. Numer. Anal.*, **30**, 630–649, (1994).